Flow Control based 5 MW Wind Turbine Enhanced Energy Production for Hydrogen Generation Cost Reduction

Aitor Saenz-Aguirre [1], Unai Fernandez-Gamiz [2,*], Ekaitz Zulueta [1], Iñigo Aramendia [2] and Daniel Teso-Fz-Betono [1]

[1] Automatic Control and System Engineering Department, University of the Basque Country (UPV/EHU), Nieves Cano, 12, 01006 Vitoria-Gasteiz, Spain; asaenz012@ikasle.ehu.eus (A.S); ekaitz.zulueta@ehu.eus (E.Z.); daniel.teso@ehu.eus (D.T.)

[2] Nuclear Engineering and Fluid Mechanics Department, University of the Basque Country (UPV/EHU), Nieves Cano, 12, 01006 Vitoria-Gasteiz, Spain; unai.fernandez@ehu.eus (U.F.); inigo.aramendia@ehu.eus (I.A.)

* Correspondence: unai.fernandez@ehu.eus; Tel.: +34-945-01-4066

Received: date; Accepted: date; Published: date

Abstract: Improving the performance and the production of renewable energy sources, especially the wind energy, is considered an attractive approach to reduce the Cost of Energy (COE) associated to the hydrogen generation process. In this context, flow control strategies have been object of detailed investigation during last years. Originally flow control devices were designed to be implemented in the aeronautical sector. Nonetheless, the optimization of the performance of the wind turbine blades with the introduction and implementation of these devices is being widely investigated these days. An analysis of the influence of implementing Vortex Generators (VGs) and Gurney Flaps (GFs) in Wind Turbine Blades (WTBs) on the Annual Energy Production (AEP) of large Horizontal Axis Wind Turbine (HAWT) is proposed in this paper. For that purpose, the Weibull distributions of annual wind speed data series of a real wind farm have been calculated, and Blade Element Momentum (BEM) based calculations have been performed to evaluate the effect of the flow control devices on the power curve and the AEP of the NREL offshore 5 MW Baseline Wind Turbine. The obtained results show an enhancement of the AEP of the turbine of 2.43% during year 2015 and 2.68% during year 2016. As a result, increments of the generated hydrogen volume larger than 130000 Nm^3 are achieved during both years with no considerable additional cost in the design of the wind turbine.

Keywords: Hydrogen Fuel Cell, Cost of Energy, Passive flow control; Vortex Generators; Gurney Flaps; AEP.

1. Introduction

Wind energy and electrical mobility systems are gaining in significance as the renewable energy generation increases due to the necessity of an energetic transition. The environmental pollution and the risk of depletion of the carbon based fuels has derived in an increase in the use of sustainable mobility and energy generation systems. One alternative to the conventional gas/diesel based vehicles are the fuel cells [1,2], in which the electrical energy is obtained through the chemical reaction of some input reactives. The most widely used fuel cell is the hydrogen fuel cell, in which oxygen and hydrogen are combined to produce electrical energy and water as the only by-product. A detailed explanation about the hydrogen as an energy source is given by Momirlana et al. [3].

The biggest drawback of the hydrogen fuel cell technology is the electrolysis reaction needed to obtain the input hydrogen. The high carbon emissions if natural gas is used as the energy source of the electrolysis process and the high costs associated to renewable energy sources as input of this reaction have avoided the industrial development of the hydrogen fuel cell technology. Nowadays, in order to reduce carbon emissions to the atmosphere renewable energy sources are intended to generate the energy necessary for the generation of the hydrogen. Autonomous hydrogen production systems based on photovoltaic energy [4], wind energy [5,6] and hybrid photovoltaic and wind energy sources [7] can be found in the literature. The improvement of the performance of the renewable energy generation systems, in this paper the wind energy, is being investigated with the objective of reducing the Cost of the Energy (COE) associated to the hydrogen generation process [8,9].

The wind energy rises as one of the most prominent renewable energy sources, being the most productive one, and reaching a degree of maturity that permits to achieve efficiency values between 96% and 99%, according to Martinez-Suarez et al. [10]. Despite this high value of efficiency, many research can be found in the literature intended to upgrade the performance of the wind turbines and increase the energetic production of these systems, making, thus, the technology more cost effective.

An overview of the literature shows the existence of several solutions ranging from the design of novel software based control strategies to the design and introduction of new hardware elements intended to improve the quality of the generated electrical power or the aerodynamic performance of the wind turbines blades. Terzi et al. [11] and Astolfi et al. [12] investigate the contribution of aerodynamic and control solutions to upgrade the power curve of a multi-megawatt wind turbine. The control of the flow across the Wind Turbine Blades (WTBs) is usually handled by flow control devices due to their excellent features for this task. Consequently, the aerodynamic performance and the energetic production of the system can be considerably enhanced. As stated by Baldacchino et al. [13], the increasing size and rated power of the actual wind turbines result in the increment of the structural and fatigue loads in the blades and the design and construction of thicker blade root sections. This new form of the blades has an undesirable effect on the aerodynamic performance of the blades due to an earlier separation of the boundary layer in the suction side of the mid-outer parts. Over the last years numerous flow control devices have been in detail investigated with the objective of overcoming the problem of the premature separation of the boundary layer. Some of them are reviewed in the work of Johnson et al. [14]. The majority of them were originally conceived for their introduction in the aeronautical sector and, nowadays, their optimization and implementation in the field of the wind energy is being faced [15,16]. The most usual classification of these devices is done according to their operating principle. Active flow control devices and passive flow control devices [17,18]. Unlike the operation of the active flow control devices, which are dependent on an external energy source, passive flow control mechanisms do not need an external excitation and more affordable form the cost point of view. Nevertheless, the performance of the passive flow control devices does not adapt to the state of the flow, but they actuate in a predefined way. Among passive flow control devices Vortex Generators (VGs) and Gurney Flaps (GFs) seem to be two of the most capable passive devices.

According to the work of Saenz-Aguirre et al. [19], a VG consists of a small vane placed normal to the surface of the airfoil in the suction side of the WTB. They are usually designed with an inclination angle with respect to the air flow direction. As described in the work of Fernandez-Gamiz et al. [20], VGs are used to modify the boundary layer motion, bringing momentum from the outer flow region into the inner flow region of the wall bounded flow, and, thus, delaying the separation of the flow from the blade surface. The effect of placing VGs in the surface of wind turbine blade has been widely studied in the literature. The most important advantage of the use of VGs is that as a consequence of the delayed boundary layer separation, the lift coefficient and the power production of the wind turbine are increased. Martinez-Suarez et al. [10] present a gain of a 0.54% and 0.67% in the mechanical torque and thrust force with the application of Rod Vortex Generators (RVG) in a NREL/NASA-Ames Phase VI rotor blade. According to Baldacchino et al. [13], an increase of the drag coefficient and the mechanical loads in the WTBs are some of the drawbacks of these flow control

devices. Regarding the design of VGs for wind turbine applications, several possibilities have been found in the literature. Lin [21] describes in his review different physical form variants that can adopt VGs, including rectangular, triangular and trapezoidal shapes. A computational model of different VG geometries placed on a flat plate is described by Gutierrez-Amo et al. [22]. Another important concept in the design of VGs is the height of the flow control devices. Fernandez-Gamiz et al. [20] stated in their work that the height of the VGs usually corresponds with the thickness of the boundary layer at the VG position. Gao et al. [23] study the effect of different VG length, height and spacing values on a DU97-W-300 airfoil via CFD simulations. In the work of Boldacchino et al. [13] the sensitivity of the airfoil in its aerodynamic performance and the effect on the loads when various design parameters are applied to the VGs are studied. An improvement of the power output and a reduction of the cyclic fatigue loads due to the use of VGs in a wind turbine is presented by Gebhardt et al. [24].

A GF is a vane positioned normal to the upper or lower side of the airfoil close to the trailing edge with a height between 1% and 2% of the airfoil chord length, see Fernandez-Gamiz et al. [25] and Saenz-Aguirre et al. [19]. Wang et al. [26] and Jeffrey et al. [27] present a detailed analysis of the performance, design and application of GFs in different airfoils. Various GF geometries have been studied in the works of van Dam et al. [28] and Chow et al. [29]. Furthermore, according to Shukla et al. [30] the implementation of GFs in NACA0012 and NACA0015 airfoils leads to an improvement in the lift coefficient, the lift force and the velocity of the blades. Storms et al. [31] present in his paper a lift increase of around 13% with negligible drag increment when an adequate sizing of GFs is adopted. Woodgate et al. [32] demonstrate the implementation and use of GFs on Computational Fluid Dynamics (CFD) simulations of blades and rotors. According to Holst et al. [33], the solution of GFs is a feasible candidate for large-scale wind turbine implementation to improve rotor aerodynamic performance and to extend the lifetime of future multi-megawatt wind turbines.

The NREL 5MW reference wind turbine of Jonkman et al. [34] is considered the basis of the future offshore Horizontal Axis Wind Turbines (HAWTs). As a result, many investigation and characterization studies about this turbine have been carried out. The WTBs considered in the present work have the same airfoils and chord configuration as the latter introduced NREL 5MW turbine. Timmer et al. [35] give detailed information and wind tunnel data on the airfoils of the DU family that have been considered for the current study.

An analysis of the influence of implementing Vortex Generators (VGs) and Gurney Flaps (GFs) in Wind Turbine Blades (WTBs) on the Annual Energy Production (AEP) of a large Horizontal Axis Wind Turbine (HAWT) and the consequent reduction of the COE of the hydrogen generation process for electric mobility applications is proposed in this paper. In fact, this analysis enables to test and quantify the performance and efficiency of flow control strategies, recently introduced in the wind energy sector, to enhance the operation of a HAWT and promote the use of the carbon emission free hydrogen as the key fuel in the future electric mobility infrastructure. For that purpose, the NASA Earth data website [36] has been used as the source of wind speed data of the years 2015 and 2016 in the Hywind Pilot Park wind farm at 3 different heights (2 m, 10 m and 50 m). Extrapolation of this data to the hub height of the NREL 5MW reference wind turbine of Jonkman et al. [34] and calculations based on Blade Element Momentum (BEM) have been performed to analyze the effect of the passive flow control devices in the performance of the wind turbine. Full details of all the experimental polar curves and the wind tunnel experiments at the Low-Speed Tunnel with a Reynolds number of 2×10^6 presented by the TU Delft University for the AVATAR project are given by Timmer et al. [35].

The current paper is structured as follows: The location of the hypothetical wind turbine that has been considered in the analysis is presented in section 2. Section 3 conducts the explanations and calculations necessary to characterize the annual wind speed data series in the location in which the wind turbine is to be placed. Section 4 presents the algorithm for the calculation of the power curve of a given wind turbine. Finally, sections 5 and 6 correspond to the current results and conclusions, respectively.

2. Wind Turbine Location

In this section, the geographical location of the hypothetical wind turbine considered in the current study is presented. The selected location for the offshore wind turbine is the Hywind Pilot Park, in the North Sea, close to the coast of Scotland, as shown in Figure 1. The wind turbine model to be installed is the NREL 5 MW, presented by Jonkman et al. [34], and which has been widely-used for offshore wind energy applications.

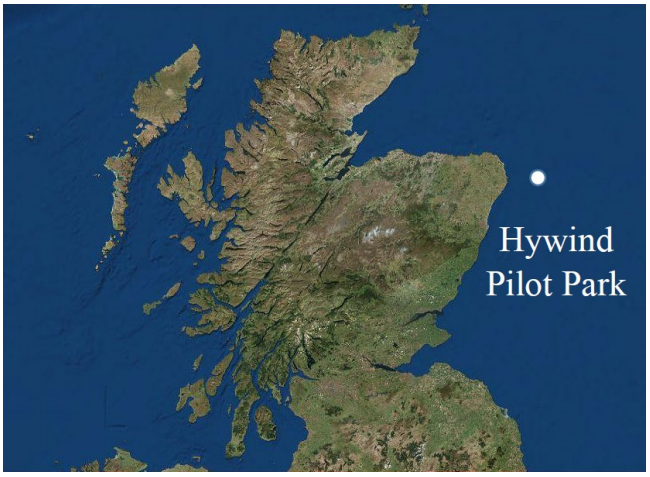

Figure 1. Hywind Pilot Park Offshore Wind Farm location

Hywind Pilot Park is a wind farm, with an installed power capacity of 30 MW and a cover area of 15 km^2. The main characteristics of this wind energy project are listed in Table 1. Hywind Pilot Park has been selected as the reference location for the analysis carried out in this paper due to the notorious growth in the development of offshore wind farms. Offshore technology, in comparison with the onshore technology, presents several important advantages. First, the absence of physical obstacles in the sea enables the wind turbine to receive stronger winds and consequently increment its generated power. Moreover, since the temperature of the sea is more stable than the temperature of the ground turbulences are less common in offshore wind farms, and the lifespan of wind turbines is increased. Finally, due to the absence of noise restrictions in the sea, the rotor can be programmed to rotate faster, and a design with less weight is possible, which is translated to a reduction of costs.

Table 1. Principal characteristics of Hywind Pilot Park wind turbines [37,38]

Designer	Siemens
Wind turbine model	SWT-6.0-154
Number of turbines	5
Wind farm rated power	30 MW
Expected life	20 years

Finally, with the objective of obtaining the wind resource data corresponding to the exact location of the wind farm, its geographical coordinates have been extracted.

- Latitude: 57.484º
- Altitude: -1.363º

3. Annual Wind Speed Characterization

3.1. Wind Speed Data, Roughness and Extrapolation

The first step of the analysis carried out in this document is the characterization of the wind speed at a height corresponding to the hub height of the considered wind turbine during a determined period of time. As it has already been stated in section 1 of this paper, the NASA Earth database [36] has been used as the source of the wind speed data corresponding to the location of the

analyzed turbine. Three different timespan values are available for the average wind speed bins stored in this database: 1 hour, 3 hours and 1 month. To the end of making the most accurate possible calculations, 1 hour averages have been chosen.

Wind speed data corresponding to the years 2015 and 2016 have been used to elaborate the wind speed profile of each one of these years. Since in the NASA Earth data database the wind speeds are only available at heights of 2 m, 10 m and 50 m, an extrapolation of these data to the hub height of 90 m, which corresponds to the hub height of the NREL 5MW turbine, is necessary. Principal characteristics of the NREL 5MW wind turbine are presented in section 4 of this document. One important factor to be considered when extrapolating wind speed data is the roughness of the earth surface. As it is exposed by Wan et al. [39], the roughness of the earth has a considerable influence on the speed of the wind in the lowest part of the atmosphere, which is commonly known as the Atmospheric Boundary Layer (ABL). The ABL is defined as the range of elevation in which wind speeds are affected by the Earth's surface, creating turbulence. As a result, the location of a wind turbine is a vital parameter when maximizing the wind speed values that are received by the generation system. The effect of ABL scenarios in the wake left by a wind turbine is studied in the work of Kabir et al. [40].

In the wind energy industry, the roughness is evaluated in meters (m) and refers to the equivalent height at which the horizontal mean wind speed value theoretically takes the value zero. Even if it is not a physical length, it is considered as an evaluation of the roughness of the surface and the wind conditions in a determined geographical location. The value of this parameter is in direct relation with the height of the elements present in the area analyzed, e.g. the value of the roughness is larger for cities with high buildings than for a flat area with no trees or buildings. Different values of the roughness length with respect to various geographical locations are listed in the work of Bañuelos-Ruedas et al [41].

Another concept related to the roughness of the earth surface is the wind shear, which is also known as the wind gradient and refers to the vertical gradient of the mean horizontal wind speed in the ABL. According to Hadi [42], the surface friction forces, which are generated by the roughness of the earth surface, slow down the wind, and a vertical gradient for the wind speed appears as a result. The bigger the value of the roughness is, the taller the wind shear will be. Empirical values of the wind shear coefficient with respect to the roughness of the terrain are presented in Table 2.

Table 2. Empirical wind shear coefficient values [39]

Terrain	Wind shear exponent
Smooth (Sea, snow, sand,)	0.10 - 0.13
Medium irregularities (Villages, farmland)	0.13 - 0.20
Irregularities (Suburbs, forests)	0.20 - 0.27
High irregularities (Tall buildings, cities)	0.27 - 0.40

The main objective of the analysis developed in this subsection is to obtain an average wind speed profile at the hub height of the analyzed NREL 5MW wind turbine. Once the wind speed profile in the location of the turbine is calculated, the AEP of the generator will be computed. The process of calculating wind speed values at a determined height starting from wind speed values at a different height is known as extrapolation.

As previously highlighted, the impact of the geographical surroundings of the wind turbine on the wind speed needs to be considered in order to extrapolate with the highest accuracy. Consequently, the roughness length has to be taken into account in the calculations. For the case of offshore wind farms, which is the case of the present study, the reduced roughness over water, and consequent small wind gradient, means that the extrapolation process should not be very affected by the surface roughness.

The performance of two different extrapolation methods, Logarithmic wind profile law and Hellman exponential law or power law, has been analyzed and compared. Thus, the one with the best performance is used for the calculations during the analysis carried out in this paper. A

comparison between these both extrapolation techniques applied to offshore wind energy applications can be found in Emeis et al. [43].

On one hand, the mathematical expression corresponding to the Logarithmic wind profile law is given in Eq. (1).

$$\frac{v}{v_0} = \frac{ln\left(\frac{H}{z0}\right)}{ln\left(\frac{H0}{z0}\right)} \quad (1)$$

where H_0 is the reference altitude, H is the altitude at which wind speed will be extrapolated, v_0 is the reference wind speed, v is the wind speed to be calculated and z_0 is the roughness length.

On the other hand, the mathematical expression corresponding to the Hellman exponential law or power law is given in Eq. (2).

$$\frac{v}{v_0} = \left(\frac{H}{H_0}\right)^{\alpha} \quad (2)$$

where H_0 is the reference altitude, H is the altitude at which wind speed will be extrapolated, v_0 is the reference wind speed, v is the wind speed to be calculated and α is the Hellman or friction coefficient.

According to the analysis carried out by Bañuelos-Ruedas et al [41] by comparing the performance of the two extrapolations methods, both are considered to give similar results in cases of not high altitudes, i.e., up to 50 m, in neutral atmospheric conditions. For altitudes higher than 50 m, the results of both methods start to differ, and, according to Hadi [42], the Hellman exponential law is considered to have a better performance.

In the present case, the wind speed values available in the NASA database, at 2 m, 10 m and 50 m high, are used. Consequently, wind speed values at 10m are considered as a reference, and wind speed values at 50 m are estimated with the previous exposed both extrapolation techniques, comparing the obtained results.

According to the values presented in Figure 2, the extrapolation process is observed to be, as expected, very similar and accurate with the both analyzed extrapolations methods for heights up to 50 m. For higher values of the height the extrapolation results start to differ from to the other. Consequently, since the hub height value of 90 m is closer to 100 m than to 20 m., for further analysis in this paper, the Hellman exponential law technique is to be used to extrapolate wind data values to the hub height of the NREL 5MW wind turbine.

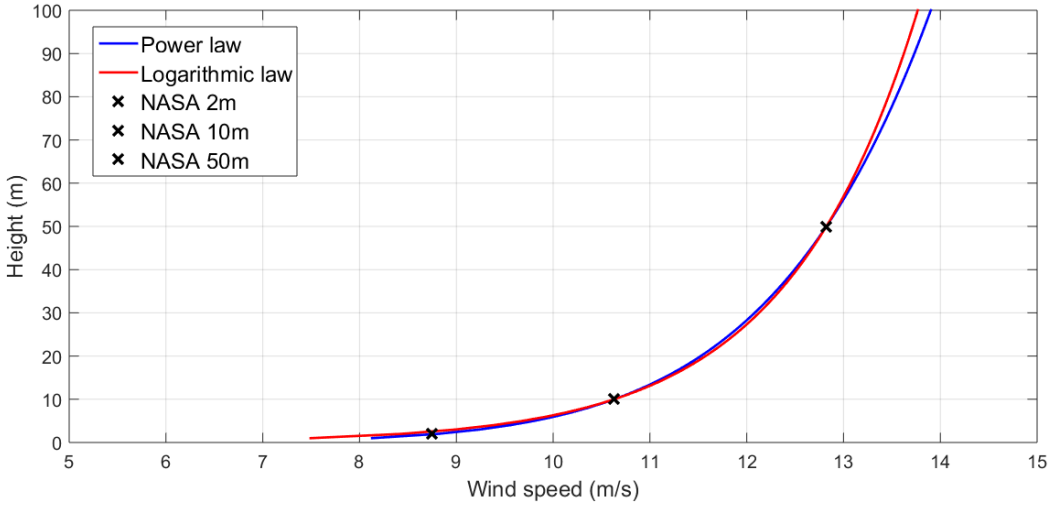

Figure 2. Comparison between analyzed extrapolation techniques

Annual wind speed profiles of the years 2015 and 2016, at 90 m of altitude, in the Hywind Pilot Park wind farm, are represented in Figure 3 and Figure 4, respectively. These wind speed data have

been correlated with the Hellmann exponential law, see Eq. (2), with the friction coefficient set to $\alpha = 0.116479$, which is calculated from the relation of the already known values of the wind speed at heights of 10m and 50m.

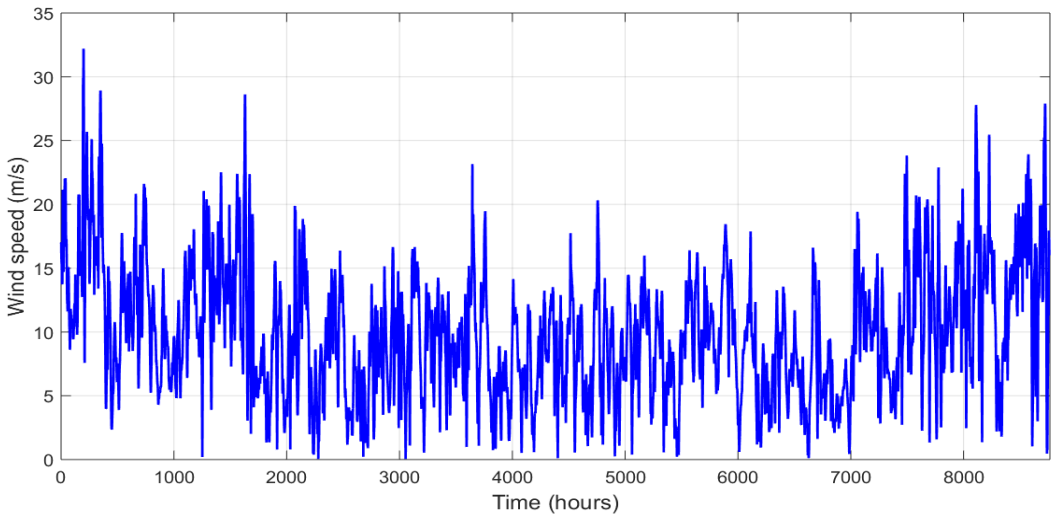

Figure 3. Profile of the wind speed in the year 2015

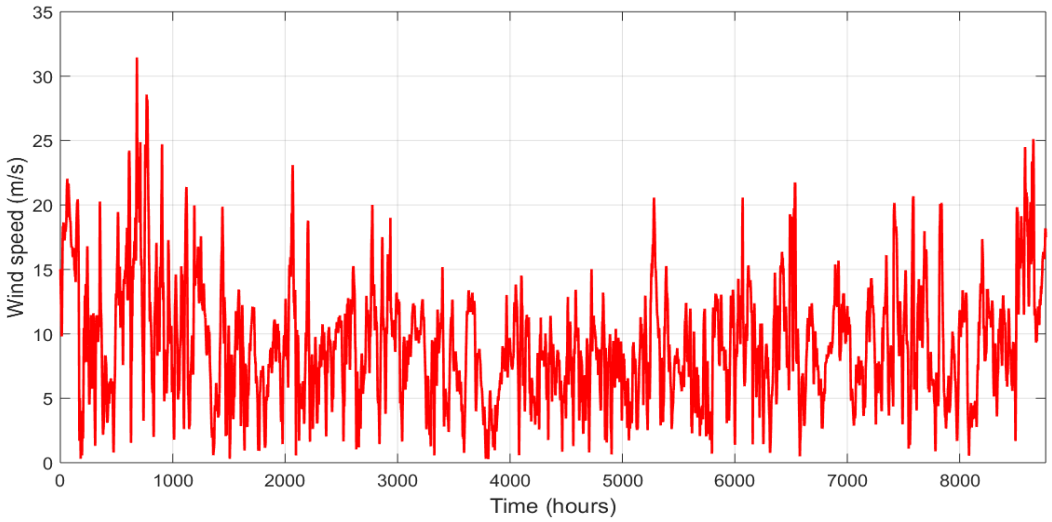

Figure 4. Profile of the wind speed in the year 2016

3.2. Wind Speed Distribution

According to Gugliani et al. [44] and Aghbalou et al. [45], the description of the wind speeds in a determined location is of great significance, since an accurate description of this probability function can derive in an optimal design of the wind turbines and a better estimation of the electrical energy generated by a wind turbine or a wind farm. In probability theory and statistics, the Weibull distribution is a continuous description of a random phenomenon in terms of the probability of events. In the wind energy field, the Weibull distribution describes the probability of a determined wind speed value to be observed in the location of a wind turbine. The sample space is formed by the wind speed value range in that particular location.

The function that describes the relative likelihood by which the value of the random variable would equal the value of the sample is the Probability Density Function (PDF). This PDF is used to specify the probability of the random variable to fall within a particular range of values, and to graphically illustrate the Weibull diagram. The PDF of a Weibull distribution is given by Eq. (3).

$$f(x) = \frac{k}{c} \cdot \left(\frac{x}{c}\right)^{k-1} e^{-\left(\frac{x}{c}\right)^{k}} \quad (3)$$

where k and c are the shape and scale parameter, respectively.

The shape parameter is a unitless number and the scale parameter is expressed in the same unit as the given sample variable. The Weibull distribution depends on the value of these two parameters. In case the shape parameter is equal to $k = 2$, the distribution is also known as the Rayleigh distribution and is frequently used by wind turbine manufacturers to estimate the energy output of wind turbines. Different methods to calculate the parameters of a Weibull distribution can be found in the scientific literature; see Mohammadi et al. [46] and Saleh et al.[47]. In this case, to form a Rayleigh distribution, the shape parameter has been set to $k = 2$ and the scale parameter c has been calculated following the moments method explained in the work of Dorvlo et al. [48], see Eq. (4).

$$c = \frac{\bar{v}}{\Gamma\left(1+\frac{1}{k}\right)} \quad (4)$$

The Weibull distributions of the annual wind speed data, at 90 m of altitude and in the Hywind Pilot Park wind farm, are illustrated for the years 2015 and 2016 in Figure 5 and Figure 6, respectively. The considered shape and scale parameters are $k = 2$ and $c = 11.18\ m/s$ for the 2015 year distribution, and $k = 2$ and $c = 10.305\ m/s$ for the 2016 year distribution.

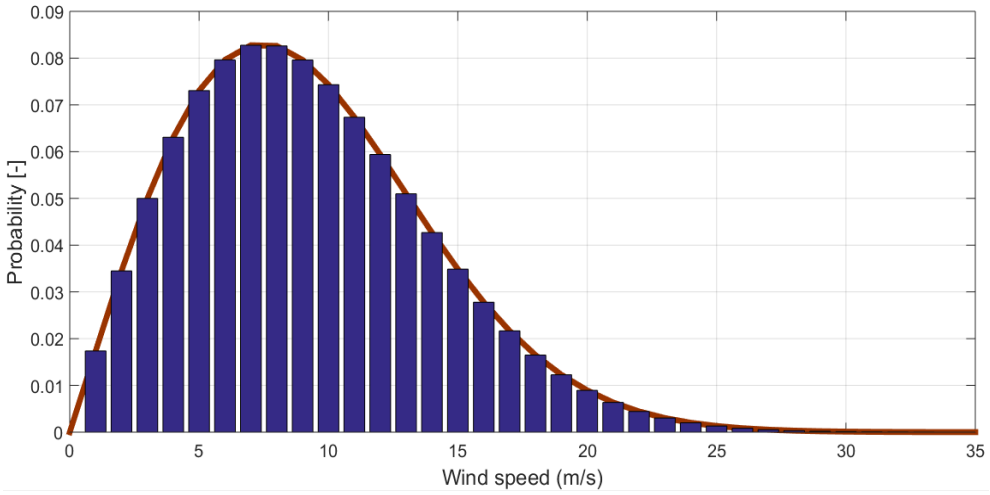

Figure 5. Weibull distribution diagram of 2015 wind speeds

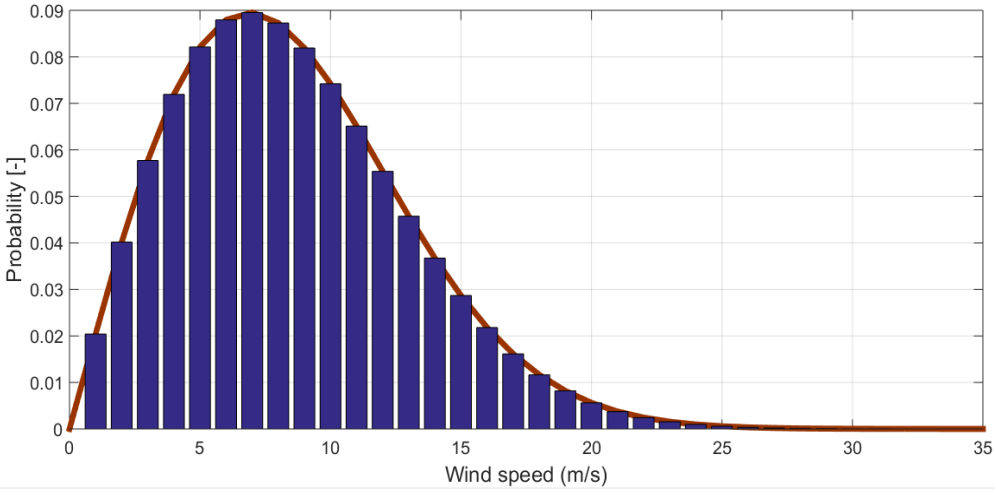

Figure 6. Weibull distribution diagram of 2016 wind speeds

Another diagram that is used to illustrate the distribution of a series of data is the Cumulative Weibull distribution, explained by Faghani et al. [49] and given by Eq. (5).

$$f(x) = 1 - e^{-\left(\frac{x}{c}\right)^k} \quad (5)$$

The Cumulative Weibull distribution is related to the conventional Weibull distribution, but it allows to observe the distribution of the wind data series form a different perspective. The sample space is set to the wind speed range in that particular location and, for the last value of this range, the unity value is reached in the cumulative function. The cumulative function must be integrated between the two edge values of the range in order to calculate the probability of a wind value range to be observed in the location of the wind turbine.

The Cumulative Weibull distributions of the annual wind speed data corresponding to the years 2015 and 2016, extrapolated at 90 m of altitude, and located in the Hywind Pilot Park, are illustrated in Figure 7.

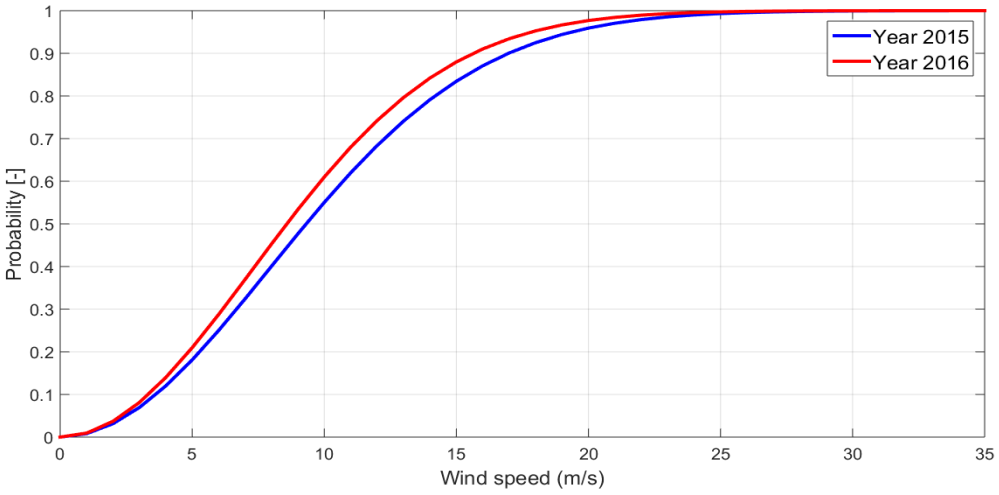

Figure 7. Cumulative Weibull distribution diagram of 2015 and 2016 wind speeds

4. Wind Turbine Performance

In this section, the performance of the wind turbine related to its aerodynamic behavior is analyzed. To that end the performance of a clean turbine, i.e., a turbine without any flow control device implemented on the blades, is compared with the performance of a turbine with passive flow control devices (VGs and GFs) by computation of its power curve. Jonkman et al. [34] described the characteristics of the NREL 5MW wind turbine, which is used as the reference turbine in the analysis performed in the current study. The principal characteristics of the NREL reference wind turbine are summarized in Table 3.

Table 3. Principal characteristics of the NREL 5W wind turbines

Turbine model	NREL 5W
Rated power	5 MW
Rotor diameter	126 m
Hub height	90 m
Cut-in wind speed	3 m/s
Rated wind speed	11.4 m/s
Cut-out wind speed	25 m/s

According to the work of Jonkman et al. [34], the blades of the NREL 5MW turbine are formed by 17 different stations, each one with its corresponding airfoil shape. The correspondence between the stations and the airfoils in the blades of the studied turbine is listed in Table 4.

Table 4. Distribution of the airfoils in the WTBs of the NREL 5MW wind turbine described in [34]

Station number	r (m)	Airfoil Type
1	2.8667	Cylinder1
2	5.6000	Cylinder1
3	8.3333	Cylinder2
4	11.7500	DU40
5	15.8500	DU35
6	19.9500	DU35
7	24.0500	DU97W300
8	28.1500	DU91W(2)250
9	32.2500	DU91W(2)250
10	36.3500	DU93W210
11	40.4500	DU93W210
12	44.5500	NACA64XX
13	48.6500	NACA64XX
14	52.7500	NACA64XX
15	56.1667	NACA64XX
16	58.9000	NACA64XX
17	61.6333	NACA64XX

The performance of a wind turbine can be calculated via different methods. Beyhaghi et al. [50] and Peng et al. [51] carried out CFD analysis to study the aerodynamic performance of a wind turbine. A computationally more economical and faster method to calculate the power curve of a wind turbine is the so-called BEM, see Hansen et al. [52]. In the analysis carried out in the present work, the power curve of the wind turbine is calculated using the BEM method presented in Fernandez-Gamiz et al. [20]. BEM based calculations have the principal advantage that they are computationally economical and fast.

The basic idea of the BEM method is the calculation of the contribution to the total of each one of the sections, independent and individually, and its posterior sum to obtain the total value of the forces generated in the WTB. In order to obtain feasible results, accurate airfoil data of the lift, drag and moment coefficients of the WTBs must be known.

According to the work of Fernandez-Gamiz et al. [20], the performance of the BEM method can be resumed with the following points:

- Initialization of axial and tangential induction parameters, a and a'.
- Calculation of the flow angle Φ.
- Calculation of the angle of attack α.
- Calculation of the lift and drag coefficients, C_L and C_D.
- Computation of the normal and tangential load coefficients, C_n and C_t.
- Recalculation of the axial and tangential induction parameters, a and a'.
- Evaluate the tolerance for axial and induction parameters.
- Computation of the power, Eq. (6), thrust, Eq. (7) and bending moment, Eq. (8).

$$P = \int_{i=0}^{R} 4\pi \cdot {r_i}^3 \cdot \rho \cdot V_0 \cdot w^2 \cdot {a'}_i \cdot (1 - a_i) \cdot F \cdot dr_i \quad (6)$$

$$T = \int_{i=0}^{R} 4\pi \cdot r_i \cdot \rho \cdot (V_0)^2 \cdot w \cdot a_i \cdot (1 - a_i) \cdot F \cdot dr_i \quad (7)$$

$$BM = \int_{i=0}^{R} 4\pi \cdot {r_i}^2 \cdot \rho \cdot (V_0)^2 \cdot w \cdot a_i \cdot (1 - a_i) \cdot F \cdot dr_i \quad (8)$$

where ρ is the density of the air, V_0 is the wind speed, w is the rotational speed of the wind turbine and F is the Prandtl's tip loss correction factor.

In the BEM algorithm, the working point of each station is assessed in order to calculate its torque contribution to the total torque developed by the WTB. To calculate these working points, an iterative algorithm is usually applied. The stop condition can be given by the maximum number of iterations or by a tolerance in the changes of the values.

In this analysis two different scenarios have been considered: A clean wind turbine, i.e. without any passive flow control device placed on the surface of the blades, and a wind turbine with flow control devices implemented on the surface of its blades.

For the first scenario, corresponding to the clean wind turbine, accurate data of the lift, drag and moment coefficients of the WTBs have been taken from the experimental work of Timmer et al. [35]. With these data BEM calculations have been performed and the value of the thrust, bending moment, power coefficient Cp and the power curve have been obtained for the whole range of wind speed values considered for the operation of the NREL 5MW wind turbine.

For the second scenario, corresponding to wind turbine with flow control devices, CFD simulations have been carried out to obtain the data of the lift, drag and moment coefficients of the WTBs. With these data BEM calculations have been performed and the value of the thrust, bending moment, power coefficient Cp and the power curve have been obtained for the whole range of the wind speed values considered for the operation of this wind turbine. As a result, an analysis of the performance of the passive flow control solution independent from the wind speed value can be carried out.

The proposed passive flow control based solution is based on a combination of VGs and GFs placed on the surface of the blades of the wind turbine, and can be described as follows:

- In the blade station 7, see Table 4, VGs have been installed in a distance of 30% of the chord length measured from the leading edge of the airfoil. No GFs have been installed in this station.
- In stations 8 and 9 VGs have been installed in a distance of 20% of the chord length measured from the leading edge of the airfoil. Moreover, GFs with a height of 2% of the chord length have been installed in the airfoil trailing edge.
- In blade stations 10 and 11, VGs have been installed in a distance of 60% of the chord length measured from the leading edge of the airfoil. No GFs have been installed in this stations.

This configuration, defined as ID25 in the work of Fernandez-Gamiz et al. [20], has been found to be the best one (as it maximizes the power coefficient Cp of the wind turbine) from a collection of 25 different possible configurations of these flow control devices applied in the WTBs.

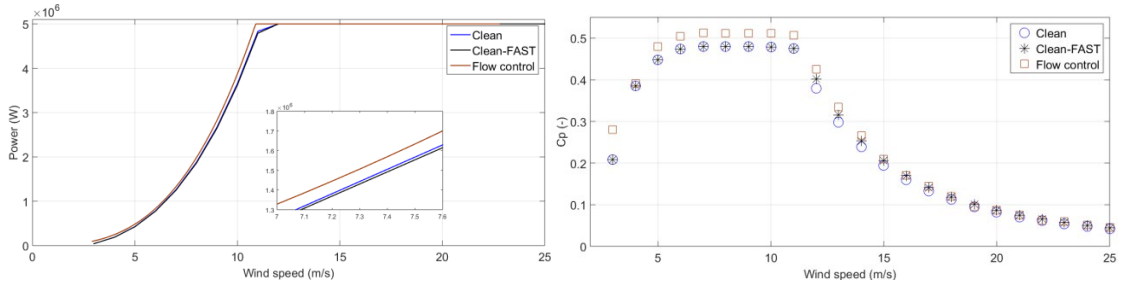

(a) (b)

Figure 8. NREL 5MW wind turbine characteristics. (a) Power curve and (b) Cp power coefficient comparison with and without implementation of passive flow control devices.

Figure 8 represents the results of the BEM calculations based on Fernandez-Gamiz et al. [20]. Figure 8(a) depicts the power curves of the wind turbine with and without passive flow control devices placed in its blades. The power coefficient Cp has also been computed in Figure 8(b) for the cases of the clean wind turbine and the case of the wind turbine with the flow control. The curve of the wind turbine with the devices for flow control follows the tendency of the clean wind turbine

curve. Nevertheless, at the wind speeds before the rated power of 5MW, the power output is enhanced due to the implementation of the flow control devices. As shown in the detailed view embedded in Figure 8(a), an increase of the power output of the wind turbine in the operating zone of partial power has been achieved by mounting passive flow control devices in the WTBs. In the rated power zone, as a result of the control system implemented in the wind turbine, the value of the generated power is kept to its rated value and the effect of the flow control devices in terms of power generation becomes negligible. The improvement of the Cp is observed in Figure 8(b) in comparison with the clean case. The power output and power coefficients of the wind turbine calculated by Jonkman et al. [34] for the same turbine have also been added in the Figure 8. The power output along the years 2015 and 2016 is illustrated in Figure 9. A clear increase in the power curve of the wind turbine with flow control devices is visible compared to the clean wind turbine at both years 2015 and 2016.

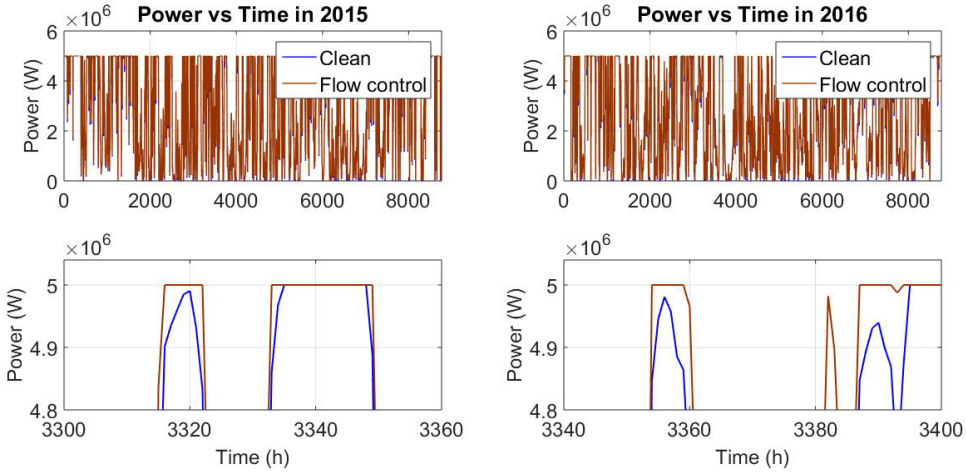

Figure 9. Power generation comparison with and without application of passive flow control devices.

In addition, in order to better characterize the effect of the passive flow control devices on the performance of the wind turbine, comparative representations of the thrust force and the bending moment in the root of the blade have been illustrated in Figure 10 and Figure 11, respectively.

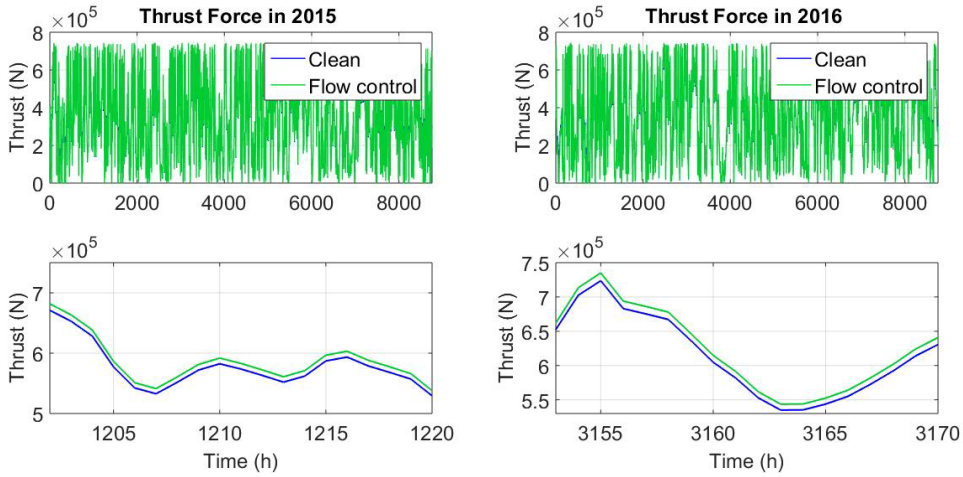

Figure 10. Thrust force comparison with and without application of passive flow control devices

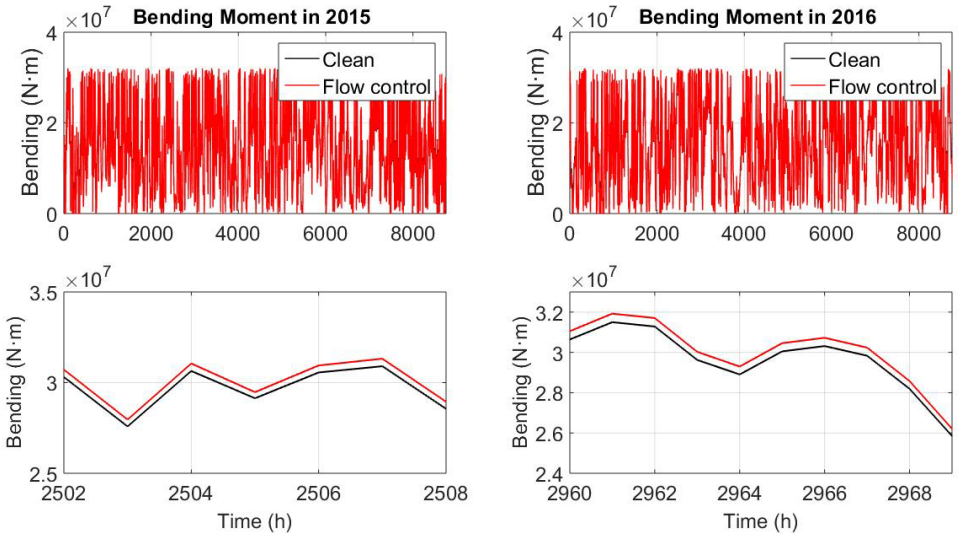

Figure 11. Bending moment comparison with and without application of passive flow control devices

As expected, the results of Figure 10 and Figure 11 show an increase of the bending moment on the root of the blade and the thrust force of the rotor of the wind turbine for wind speed values below rated (see zoomed views of Figure 10 and Figure 11) with the application of the flow control based solution into the WTBs.

5. Wind Turbine Annual Energy Production

In this section, the AEP value of a clean turbine is calculated and compared with the AEP value of a turbine equipped with VGs and GFs in its airfoils, i.e., the effect of placing passive flow control devices on the AEP of a NREL 5 MW turbine is analyzed.

In order to compute AEP value of the wind turbine, the Weibull distribution of the annual wind speed data and the power curve of the turbine have been first obtained in sections 3 and 4. Using these two functions, the AEP of the wind turbine can be easily computed with the expressions given in Eq. (9)-(10).

$$P_{average} = \frac{\sum_{j=1}^{j=Nbins} P(V_{0,j}) \cdot N(V_{0,j})}{\sum_{j=1}^{j=Nbins} N(V_{0,j})} \quad \text{(W)} \tag{9}$$

$$AEP = P_{average} \cdot 8760 \quad \text{(W·h)} \tag{10}$$

$N(V_{0,j})$ represents the number of samples for each bin, V_0 the wind speed and *8760* is the number of hours per year. If the calculation given in Eq. (9) is performed, the mean power of the NREL 5MW wind turbine is calculated using its power curve and the probability function of the wind speed in its location. If the mean power value is multiplied by the number of hours in a whole year, see Eq. (10), the AEP value for that year is obtained. Using the AEP value of the clean NREL 5MW wind turbine as a reference, the increment or decrement of the AEP value of the NREL 5MW wind turbine equipped with the passive flow control devices can be calculated.

One important aspect regarding VGs and GFs is their facility to be mounted on the blades, as they can be placed on them after the blade is already fabricated, which means that no interference is necessary with the usual fabrication process of the blades.

Table 5. Annual Energy Production increase with the application of passive flow control devices

ANNUAL ENERGY PRODUCTION			
Year	**Clean (kW·h)**	**Flow control (kW·h)**	**ΔAEP (%)**
2015	$2.4708 \cdot 10^7$	$2.5309 \cdot 10^7$	2.4329
2016	$2.4371 \cdot 10^7$	$2.5023 \cdot 10^7$	2.6773

According to the results, presented in Table 5 , the AEP of the NREL 5MW wind turbine equipped with the VGs and the GFs is incremented by a 2.43% in year 2015 and a 2.68% in year 2016 in comparison to the same wind turbine without these flow control devices located in the Hywind Pilot Park wind farm. The bigger AEP increase in the case of year 2016 in comparison to year 2015 can be explained with a higher probability of wind speed values above the rated one during year 2015. During these high wind speed intervals the control system of the wind turbine keeps the value of the generated power to its rated value and the effect of the passive flow control devices disappears. This can be confirmed with the Weibull distributions shown in Figure 5 and Figure 6. In both cases the power enhancement is bigger than the one presented by Ebrahimi et al. [53] with the utilization of plasma actuators in the same wind turbine. In that case the power increase is limited to 0.85% in the best case.

If it is considered that the wind farm is connected to the grid, the obtained AEP increment with the utilization of VGs and GFs can be transformed to economical profits in order to better evaluate the impact of implementing these passive flow control devices on an offshore wind turbine. Due to oscillations in the price of the energy in the regulated market, two different prices are considered in this analysis (3 ct/KW·h and 5 ct/KW·h), as it is also considered in the work of Schramm et al. [54]. Table 6 shows the results in terms of the economical profits for those different scenarios at the years 2015 and 2016.

Table 6. Annual economical profit with application of passive flow control devices

Economical profit (€)		
Year	**3 ct/kW·h**	**5 ct/kW·h**
2015	18030 €	30050 €
2016	19575 €	32625 €

In the same way, if it is considered that the wind farm is not connected to the grid, but it corresponds to a Power to Gas plant, i.e. its objective is the large-scale production of hydrogen by electrolysis, the obtained AEP increment with the utilization of VGs and GFs can be transformed to a generated additional hydrogen volume. For these calculations, the technical characteristics of the commercial large-scale electrolyser *McLyzer 400-30* designed by the company *McPhy* and installed in a 4 MW Power to Gas wind farm [55] in Hebei, China has been considered. The energy consumption of this electrolyser is 4.5 kW·h/Nm^3. The obtained results in terms of annual generated hydrogen volume are presented in Table 7. The second column shows the volume of hydrogen, in normal conditions of this gas, generated by the wind farm in each one of the analyzed years with no passive flow control devices implemented in the WTBs. The third column shows the volume of hydrogen, in normal conditions of this gas, generated by the wind farm in each one of the analyzed years with VGs and GFs implemented in the WTBs. The last column corresponds to the generated additional hydrogen volume with the implementation of the passive flow control devices based solution.

Table 7. Annual generated hydrogen volume increase with the application of passive flow control devices

ANNUAL HYDROGEN GENERATION			
Year	**Clean (Nm^3)**	**Flow control (Nm^3)**	**ΔV_{H_2} (Nm^3)**
2015	$5.4907 \cdot 10^6$	$5.6242 \cdot 10^6$	133500
2016	$5.4158 \cdot 10^6$	$5.5607 \cdot 10^6$	144998

The annual economical profits and the annual generated additional hydrogen volume in Table 6 and Table 7, respectively, indicate the relevancy of implementing passive flow control devices in the blades of a wind turbine. On the one hand, if the wind farm is connected to the grid, with possible annual economical profits of around 30.000 € the time necessary to compensate the initial inversion for the installation of a wind turbine or a wind farm can be reduced, and, hence, the time to start making benefits and the COE are reduced, which is a considered to be a key factor for the promotion of the renewable energies. On the other hand, if the wind farm is a Power to Gas plant, the generated additional hydrogen volume is increased by around 150000 Nm^3 with no considerable variation in the price of the wind farm. This additional hydrogen could cover a journey of 100 km of almost 1 million of hydrogen cars without extra cost. Hence, a reduction of the associated COE and a significant progress of the hydrogen generation process are to be achieved.

6. Conclusions

The effect of implementing passive flow control devices, VGs and GFs, on the AEP of a multi megawatt HAWT has been analyzed in this paper. The Weibull distributions of the annual wind speed data corresponding to a real offshore wind farm for two different years have been calculated and BEM based computations have been performed to obtain the power curve of a reference wind turbine model in different scenarios and study the influence of mounting VGs and GFs on the performance of the turbine.

According to the obtained results:

- In the selected location of the wind turbine, an increment of 2.43% and 2.68% is achieved in the AEP of the turbine in the years 2015 and 2016, respectively, with the introduction of the flow control devices.
- These increments of 2.46% and 2.68% can be transformed to economical profits of 30050 € and 46900 € or generated additional hydrogen volumes of 133500Nm^3 and 208400 Nm^3 for each one of the analyzed years.
- The economical profits permit to reduce the time necessary to compensate the initial inversion and start making benefits. The generated additional hydrogen volume enable to increase the efficiency of the hydrogen generation process. Either way an important reduction of the COE associated to the energy generation process is achieved, which is of great importance for the future development of the electric vehicle industry.

Regarding the performance of the wind turbine with the VGs and the GFs placed on the blades, an increment of the power of the system and the thrust force, at expenses of an increase of the bending moment at the root of the WTBs, has been observed. The increased bending moment derives in higher loads experienced by the structural components of the turbine.

Acknowledgments: This project has been financed by the Government of the Basque Country through the SAIOTEK (S-PE11UN112) research program and by the Foundation VITAL Fundazioa, Grant No.: FP18/36.

References

[1] Marbán G., Valdés-Solís T.: Towards the hydrogen economy?, Int J Hydrogen Energy, 2007, 32, (12), pp. 1625.

[2] Balat M.: Potential importance of hydrogen as a future solution to environmental and transportation problems, Int J Hydrogen Energy, 2008, 33, (15), pp. 4013.

533 [3] Momirlana M., Veziroglub T.N.: The properties of hydrogen as fuel tomorrow in
534 sustainable energy system for a cleaner planet, International Journal of Hydrogen Energy,
535 2005, 30, (7), pp. 795-802.

536 [4] Kovac A.: Autonomous hydrogen production system, International Journal of Hydrogen
537 Energy, 2015, 40, (24), pp. 7465-7474.

538 [5] Dutton A.G., Bleijsb J.A.M., Dienhartc H.*, et al*.: Experience in the design, sizing,
539 economics, and implementation of autonomous wind-powered hydrogen production
540 systems, International Journal of Hydrogen Energy, 2000, 25, (8), pp. 705-722.

541 [6] Ayodele T.R., Munda J.L.: Potential and economic viability of green hydrogen
542 production by water electrolysis using wind energy resources in South Africa, Int J
543 Hydrogen Energy, 2019, 44, (33), pp. 17669.

544 [7] Agbossou K., Chahine R., Hamelin J.*, et al*.: Renewable energy systems based on
545 hydrogen for remote applications, Journal of Power Sources, 2001, 96, (1), pp. 168-172.

546 [8] Cetinkaya E., Dincer I., Naterer G.F.: Life cycle assessment of various hydrogen
547 production methods, Int J Hydrogen Energy, 2012, 37, (3), pp. 2071.

548 [9] Fang R.: Life cycle cost assessment of wind power–hydrogen coupled integrated energy
549 system, Int J Hydrogen Energy, 2019, 44, (56), pp. 29399.

550 [10] Suarez J.M., Flaszynski P., Doerffer P.: Application of rod vortex generators for flow
551 separation reduction on wind turbine rotor, Wind Energy, 2018, 21, (11), pp. 1202-1215.

552 [11] Terzi L., Lombardi A., Castellani F., Astolfi D.: Innovative methods for wind turbine
553 power curve upgrade assessment, J.Phys., Conf.Ser.(UK), 2018, 1102, pp. 012036 (11 pp.);
554 012036(11.)-012036 (11 pp.).

555 [12] Astolfi D., Castellani F., Terzi L.: Wind Turbine Power Curve Upgrades, Energies,
556 May 2018, 11, (5), pp. 1300.

557 [13] Baldacchino D., Ferreira C., De Tavernier D., Timmer W.A., van Bussel G.J.W.:
558 Experimental parameter study for passive vortex generators on a 30% thick airfoil, Wind
559 Energy, 2018, 21, (9), pp. 745-765.

560 [14] Johnson Scott J., van Dam C.P., Berge Dale E.: Active Load Control Techniques for
561 Wind Turbines (SANDIA REPORT, SAND2008-4809 August, 2008).

562 [15] Fernandez-Gamiz U., Marika Velte C., Rethore P.-., Sorensen N.N., Egusquiza E.:
563 Testing of self-similarity and helical symmetry in vortex generator flow simulations, Wind
564 Energy, 2016, 19, pp. 1043-1052.

[16] Martinez-Filgueira P., Fernandez-Gamiz U., Zulueta E., Errasti I., Fernandez-Gauna B.: Parametric study of low-profile vortex generators, Int J Hydrogen Energy, 2017, 42, (28), pp. 17700-17712.

[17] Aramendia-Iradi I., Fernandez-Gamiz U., Sancho-Saiz J., Zulueta-Guerrero E.: State of the art of active and passive flow control devices for wind turbines, 2016, DYNA, 91(5). 512-516.

[18] Aramendia I., Fernandez-Gamiz U., Ramos-Hernanz J., Sancho J., Lopez-Guede J., Zulueta E.: Flow Control Devices for Wind Turbines, in Bizon N., Mahdavi Tabatabaei N., Blaabjerg F., Kurt E. (Eds.): Energy Harvesting and Energy Efficiency: Technology, Methods, and Applications (Springer International Publishing, Cham, 2017, pp. 629-655.

[19] Saenz-Aguirre A., Fernandez-Resines S., Aramendia I.*, et al*.: 5 MW Wind Turbine Annual Energy Production Improvement by Flow Control Devices, Proceedings, 2018, 2, pp. 1452.

[20] Fernandez-Gamiz U., Zulueta E., Boyano A., Ansoategui I., Uriarte I.: Five Megawatt Wind Turbine Power Output Improvements by Passive Flow Control Devices, Energies, 2017, 10, (6), pp. 742.

[21] Lin J.C.: Review of research on low-profile vortex generators to control boundary-layer separation, 2002, 38 (4-5), pp. 389-420.

[22] Gutierrez-Amo R., Fernandez-Gamiz U., Errasti I., Zulueta E.: Computational Modelling of Three Different Sub-Boundary Layer Vortex Generators on a Flat Plate, Energies, 2018, 11, (11).

[23] Gao L., Zhang H., Liu Y., Han S.: Effects of vortex generators on a blunt trailing-edge airfoil for wind turbines, Renewable Energy, 2015, 76, pp. 303-311.

[24] Gebhardt C.G., Preidikman S., Massa J.C.: Numerical simulations of the aerodynamic behavior of large horizontal-axis wind turbines, International Journal of Hydrogen Energy, 2010, 35, (11), pp. 6005-6011.

[25] Fernandez-Gamiz U., Gomez-Marmol M., Chacon-Rebollo T.: Computational Modeling of Gurney Flaps and Microtabs by POD Method, Energies, 2018, 11, (8), pp. 2091.

[26] Wang J.J., Li Y.C., Choi K.-.: Gurney flap—Lift enhancement, mechanisms and applications, Progress in Aerospace Sciences, 2008, 44, pp. 22-47.

[27] Jeffrey D., Zhang X., Hurst D.W.: Aerodynamics of Gurney flaps on a single-element high-lift wing, J.Aircr., 2000, 37, (2), pp. 295-301.

598 [28] van Dam C.P., Chow R., Zayas J.R., Berg D.A.: Computational Investigations of
599 Small Deploying Tabs and Flaps for Aerodynamic Load Control, Journal of Physics,
600 Conference series: The Science of Making Torque from Wind, 2007, 75.

601 [29] Chow R., van Dam C.P.: On the temporal response of active load control devices,
602 Wind Energy, 2010, 13, (2-3), pp. 135-149.

603 [30] Shukla V., Kaviti A.K.: Performance evaluation of profile modifications on straight-
604 bladed vertical axis wind turbine by energy and Spalart Allmaras models, Energy, 2017,
605 126, pp. 766-795.

606 [31] Storms B.L., Jang C.S.: Lift Enhancement of an Airfoil using a Gurney Flap and
607 Vortex Generators, J.Aircr., 1994, 31, (3), pp. 542-547.

608 [32] Woodgate M.A., Pastrikakis V.A., Barakos G.N.: Rotor Computations with Active
609 Gurney Flaps, In: Braza M., Bottaro A., Thompson M. (eds) Advances in Fluid-Structure
610 Interaction. Notes on Numerical Fluid Mechanics and Multidisciplinary Design, vol 133.
611 Springer, Cham, 2016.

612 [33] Holst D., Bach A.B., Nayeri C.N., Paschereit C.O., Pechlivanoglou G.: Wake Analysis
613 of a Finite Width Gurney Flap, Journal of Engineering for Gas Turbines and Power-
614 Transactions of the Asme, 2016, 138, (6), pp. 062602.

615 [34] Jonkman J.M., Butterfield S., Musial W., Scott G.: Definition of a 5MW Reference
616 Wind Turbine for Offshore System Development, National Renewable Energy Laboratory
617 (NREL), 2009.

618 [35] Timmer W., van Rooij R.: Summary of the Delft University wind turbine dedicated
619 airfoils, Journal of Solar Energy Engineering-Transactions of the Asme, 2003, 125, (4), pp.
620 488-496.

621 [36] https://earthdata.nasa.gov/.

622 [37] Statoil.: Hywind Scotland Pilot Park. Environmental Statement Non Technical
623 Summary, April 2015.

624 [38] Statoil.: Hywind Scotland Pilot Park. The world's first floating wind farm, All Energy,
625 2016.

626 [39] Wan S., Cheng L., Sheng X.: Effects of Yaw Error on Wind Turbine Running
627 Characteristics Based on Equivalent Wind Speed Model, Energies, 2015, 8, pp. 6286-6301.

628 [40] Kabir I.F.S.A., Ng E.Y.K.: Effect of different atmospheric boundary layers on the
629 wake characteristics of NREL phase VI wind turbine, Renewable Energy, 2019, 130, pp.
630 1185-1197.

631 [41] Banuelos-Ruedas F., Rios-Marcuello S., Angeles-Camacho C.: Methodologies Used in
632 the Extrapolation of Wind Speed Data at Different Heights and Its Impact in the Wind
633 Energy Resource Assessment in a Region, Methodologies Used in the Extrapolation of
634 Wind Speed Data at Different Heights and Its Impact in the Wind Energy Resource
635 Assessment in a Region. Potential Estimation and Siting Assessment, 2011.

636 [42] Hadi F.A.: Diagnosis of the Best Method for Wind Speed Extrapolation, International
637 Journal of Advanced Research in Electrical, Electronics and Instrumentation Engineering,
638 2015, 4, (10).

639 [43] Emeis S., Turk M.: Comparison of Logarithmic Wind Profiles and Power Law Wind
640 Profiles and their Applicability for Offshore Wind Profiles, February 2007, pp. 61-64.

641 [44] Gugliani G.K., Sarkar A., Ley C., Mandal S.: New methods to assess wind resources
642 in terms of wind speed, load, power and direction, Renewable Energy, 2018, 129, pp. 168-
643 182.

644 [45] Aghbalou N., Charki A., Elazzouzi S.R., Reklaoui K.: A probabilistic assessment
645 approach for wind turbine-site matching, International Journal of Electrical Power &
646 Energy Systems, 2018, 103, pp. 497-510.

647 [46] Mohammadi K., Alavi O., Mostafaeipour A., Goudarzi N., Jalilvand M.: Assessing
648 different parameters estimation methods of Weibull distribution to compute wind power
649 density, Energy Convers Manage, 2016, 108, pp. 322-335.

650 [47] Saleh H., Aly A.A.E.-., Abdel-Hady S.: Assessment of different methods used to
651 estimate Weibull distribution parameters for wind speed in Zafarana wind farm, Suez Gulf,
652 Egypt, Energy, 2012, 44, pp. 710-719.

653 [48] Dorvlo A.S.S.: Estimating wind speed distribution, Energy Conversion and
654 Management, 2002, 43, (17), pp. 2311.

655 [49] Faghani G.R., Ashrafi Z.N., Sedaghat A.: Extrapolating wind data at high altitudes
656 with high precision methods for accurate evaluation of wind power density, case study:
657 Center of Iran, Energy Conversion and Management, 2018, 157, pp. 317-338.

658 [50] Beyhaghi S., Amano R.S.: A parametric study on leading-edge slots used on wind
659 turbine airfoils at various angles of attack, Journal of Wind Engineering and Industrial
660 Aerodynamics, 2018, 175, pp. 43-52.

661 [51] Peng H.Y., Lam H.F., Liu H.J.: Numerical investigation into the blade and wake
662 aerodynamics of an H-rotor vertical axis wind turbine, Journal of Renewable and
663 Sustainable Energy, 10.1063/1.5040297, (5).

664 [52] Hansen M.O.L., S\orensen J.N., S Voutsinas, S\orensen N.N., Aagaard Madsen
665 Helge.: State of the art in wind turbine aerodynamics and aeroelasticity, Prog.Aerospace
666 Sci., 2006, 42, pp. 285-330.

667 [53] Ebrahimi A., Movahhedi M.: Power improvement of NREL 5-MW wind turbine using
668 multi-DBD plasma actuators, 2017, 146, pp. 96-106.

669 [54] Schramm M., Rahimi H., Stoevesandt B., Tangager K.: The Influence of Eroded
670 Blades on Wind Turbine Performance Using Numerical Simulations, Energies, 2017, 10,
671 (9), pp. 1420.

672 [55] Fuel Cells B.: McPhy delivers 4 MW of hydrogen production to China for P2G
673 application with wind farm, Elsevier, 2017, 6, pp. 1.

674
675